IEEE Access
Multidisciplinary | Rapid Review | Open Access Journal

Received September 4, 2017, accepted October 9, 2017, date of publication October 25, 2017, date of current version March 9, 2018.

Digital Object Identifier 10.1109/ACCESS.2017.2766231

A Wideband Quad-Polarization Reconfigurable Metasurface Antenna

JUN HU[1], (Student Member, IEEE), GUO QING LUO[2], (Member, IEEE), AND ZHANG-CHENG HAO[1], (Senior Member, IEEE)

[1]State Key Laboratory of Millimeter Waves, Southeast University, Nanjing 210096, China
[2]School of Electronics and Information, Institute of Antennas and Microwave Technology, Hangzhou Dianzi University, Hangzhou 310018, China

Corresponding author: Zhang-Cheng Hao (zchao@seu.edu.cn)

This work was supported in part by the National Natural Science Foundation of China under Grant 61471118 and in part by the Scientific Research Foundation of Graduate School of Southeast University under Grant YBJJ1712.

ABSTRACT A low-profile wideband metasurface antenna with quad-polarization reconfiguration ability is presented in this paper. The proposed metasurface antenna is composed of a square patch, a metasurface formed by a lattice of 4 × 4 periodic metal plates, and four switchable feeding probes connected with two designed single-pole double-throws switches. By properly selecting the feeding probes, the polarization of the metasurface antenna can be dynamically reconfigured among four polarization states, i.e., *x*-direction linear polarization, *y*-direction linear polarization, left-hand circular polarization, and right-hand circular polarization. To validate the proposed concept, a prototype operating at 5.6 GHz with a relatively height of 0.067 λ_0 (λ_0 is the operating wavelength in free space) is designed, fabricated, and measured. The measured results show that both the 10-dB impedance bandwidths and the 3-dB axial ratio bandwidths are wider than 5.1–6.0 GHz for the linear and circular polarization states. The measured maximum gains are 9.39 dBic and 9.85 dBi for the circular polarization states and the linear polarization states, respectively. The simulation and experimentation verify that the proposed antenna can achieve quad-polarization reconfigurable features in a wide frequency band, which indicate the good performance of the proposed polarization reconfigurable metasurface antenna.

INDEX TERMS Polarization reconfigurable, wideband, low profile, metasurface antenna, PIN diode.

I. INTRODUCTION

In recent years, research on reconfigurable antennas, including pattern [1], [2], frequency [3], and polarization [4], [5] diversities, has received increasing attention in modern wireless communication systems. In particular, polarization reconfigurable antennas are desirable for many applications due to the ability to reconfigure the polarization states among dual orthogonal linear polarization (LP), left-hand circular polarization (LHCP) and right-hand circular polarization (RHCP), which has the advantages of improving system performance through eliminating multipath fading [6], a frequency reuse [7], and avoiding polarization mismatch.

Recently, a number of polarization reconfigurable antennas [8]–[18] have been developed for wireless communication. Generally, polarization reconfigurable antennas can be realized by two kinds of technology. The first one is to introduce switchable perturbation segments in the antenna's internal structure directly, as in [9]–[12], while the other one is to adopt a switchable feeding network, as in [13]–[15]. In [9]–[11], the current distributions for different polarization states on the radiation element were controlled by using RF switches. However, the dc bias circuit for RF switches was designed on the top layer, which may affect seriously the antenna performance. In [14], the electrically controllable phase-shifting was introduced in the feeding network. By controlling the states of feeding network, the polarization of the proposed antenna can be switched among LP, LHCP and RHCP, or dual orthogonal linear polarization and dual orthogonal circular polarization, such as in [19]–[23]. Nevertheless, these antennas have a complex feeding network or multi-ports input, and their operating bandwidths are narrow.

In our previous work [24], a wideband antenna array with quad-polarization reconfigurable ability was realized using four LP antenna elements, in which each polarization states are formed by four LP antenna elements. But as a common issue, the cross polarization levels of the array for the four polarization states are high in the diagonal plane. By using the similar schematic in [24], the four radiating elements

are arranged clockwise or anticlockwise and fed with equal amplitude and 90-degree phase difference for achieving CP waves. Due to the larger space between antenna elements, the condition, i.e., equal amplitude and 90-degree phase difference, is not satisfied strictly in the diagonal plane, which may decrease the cross polarization performance. To address this problem, a single antenna element with four feeding probes can be used to replace the four single-feeding radiating elements.

In this paper, we present a wideband quad-polarization reconfigurable metasurface antenna which consists of a square patch, a metasurface layer and four feeding probes with a switchable feeding network. By properly selecting the feeding probes, the proposed antenna can work at four polarization states, namely, X-LP, Y-LP, LHCP, and RHCP. The rest of this paper is organized as follows. Section II shows the design of the proposed metasurface antenna in detail. Both the simulated and experimental results are presented for comparison in Section III. Finally, the conclusions are drawn in Section IV.

II. ANTENNA GEOMETRY AND OPERATION PRINCIPLE

A. CONFIGURATION OF ANTENNA

The geometrical configuration of the proposed metasurface antenna is shown in Fig. 1. The whole antenna structure is composed of three layers: the metasurface layer, the driven patch layer, and the feeding network layer, which are designed on two 0.508-mm thickness RO4350 substrates ($\varepsilon_r = 3.66$ and $\tan\delta = 0.004$ at 10 GHz), and a 0.508-mm thickness TLY-5 substrate ($\varepsilon_r = 2.2$ and $\tan\delta = 0.0009$ at 10 GHz), respectively, as shown in Fig. 1(a). The height of the air gap between the metasurface layer and the driven patch layer is h_4. The driven patch layer and the feeding network layer are connected by using a piece of bonding film, which is a 0.1-mm thickness RO4450 substrate ($\varepsilon_r = 3.48$ and $\tan\delta = 0.004$ at 10 GHz).

The metasurface layer is formed by a lattice of 4×4 periodic metal plates with periodicity p and a gap g between two adjacent plates. The driven patch layer consists of a square patch with a width of wp, and four feeding probes which are connected using two designed single-pole double-throws (SPDT) switches. Four microstrip stubs with a dimension of $Wm \times Lm$, are connected with the driven patch through PIN diodes for probe feed [25]. The driven patch is fed by a probe through a circular aperture at the ground plane. The diameters of the hole and the feeding probe are denoted as d, ds, respectively. The switchable feeding network is composed of a 2-way power divider and two SPDT switches, which are designed by using PIN diodes (MADP-000907-14020) from MACOM Company [26]. The PIN diodes can be activated by a dc voltage through a bias circuit, which uses a thin microstrip line as inductor and a sector microstrip as short capacitor. A shorting pin in the center of the driven patch is used to connect the patch the ground plane for the dc bias. The width w_{50} of the input microstrip line is designed

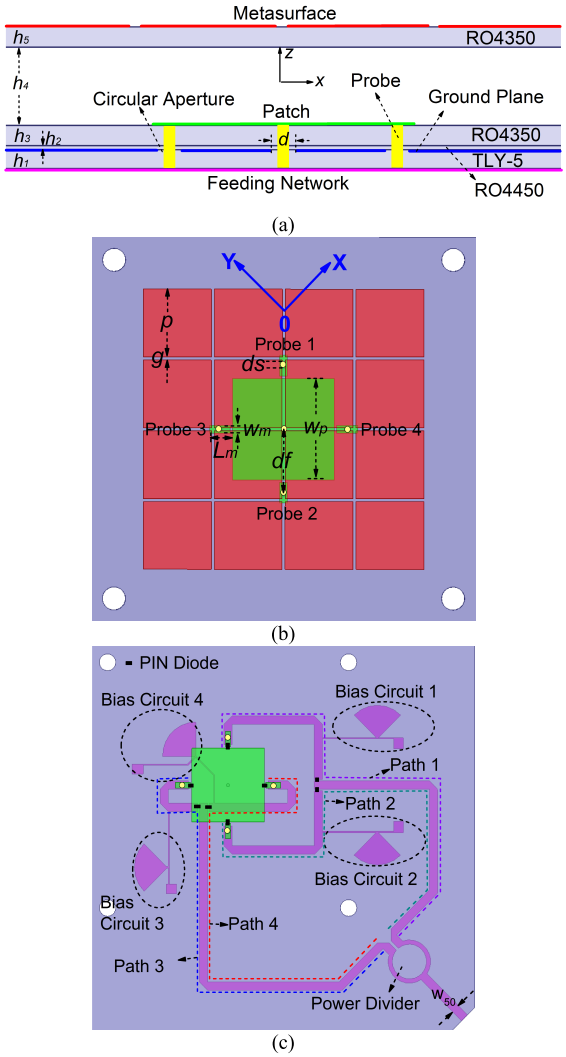

FIGURE 1. Geometrical configuration of the proposed wideband quad-polarization reconfigurable metasurface antenna. (a) Side view. (b) Top view. (c) Bottom view.

with a characteristic impedance of 50-ohm. To arrange the dc bias circuit, the size of the feeding network is deliberately designed a little larger than that of the metasurface layer, which may be reduced by using lumped elements in the design.

B. OPERATION PRINCIPLE

The initial size of the square driven patch can be determined by the following formula:

$$\mathrm{Wp} = \frac{\lambda 0}{2\sqrt{\varepsilon}} \tag{1}$$

where λ_0 is the wavelength of the operation frequency in the air so that the patch resonates at TM_{01} mode, and ε is the relatively permittivity of the substrate. To broaden the operating bandwidth, the metasurface layer is adopted in the design and loaded on the driven patch for introducing extra resonances generated by surface waves propagating on the

TABLE 1. Polarizations by different feeding ports.

Path 1	Path 2	Path 3	Path 4	Polarization states
Probe 1	Probe 2	Probe 3	Probe 4	
ON	OFF	ON	OFF	Y-LP
ON	OFF	OFF	ON	LHCP
OFF	ON	OFF	ON	RHCP
OFF	ON	ON	OFF	X-LP

TABLE 2. Geometrical parameters of the proposed antenna (mm).

Parameter	Value	Parameter	Value
h_1	0.508	g	0.4
h_2	0.1	d	0.8
h_3	0.508	ds	0.4
h_4	2	df	8.2
h_5	0.508	Lm	3
p	8.8	Wm	1
Wp	13.1	w_{50}	1.5

finite-size metasurface. Considering the finite-size metasurface as a cavity, the resonance of surface wave is governed by the following equation [27], [28]:

$$\beta_{sw} = \frac{\pi}{L} \tag{2}$$

where β_{sw} represents the propagation constant of the surface wave, and L (equal $4 \times (p + g)$ here) is the total length of the metasurface structure.

The four feeding probes can be switched by controlling the states of the two SPDT switches. As shown in Fig. 1(c), the signal paths for the four ports are denoted as Path 1-4, respectively. The lengths of Path 1-3 are equal, and $\lambda_g/4$ shorter than that of Path 4, where λ_g is the wavelength of guided wave in the microstrip. By properly controlling the states of the two SPDT switches, the proposed antenna can work at four polarization modes. For example, when Probe 1 and 3 are selected, the antenna will radiate a LP wave in the far-field due to the equal amplitude and phase. A CP wave can be produced by choosing the Probe 1 and 4 (or Probe 2 and 4) because of 90-degree phase-shift. All four polarization states and the corresponding states of the four probes are summarized in Table I.

The proposed antenna has been simulated and optimized by using a full-wave commercial software, i.e., the HFSS simulator, and the final design values are listed in Table II. In order to clearly see the operation mechanism, the full-wave simulated 5.6 GHz vector surface current distributions on the metasurface and 3-D radiation patterns for the four polarization states are illustrated in Fig. 2 and Fig. 3, respectively. From Fig. 2, it can be clearly observed that the polarization of the proposed antenna can be switched among the four modes by selecting properly feeding probes. The simulated 5.6 GHz normalized radiation patterns in the diagonal plane

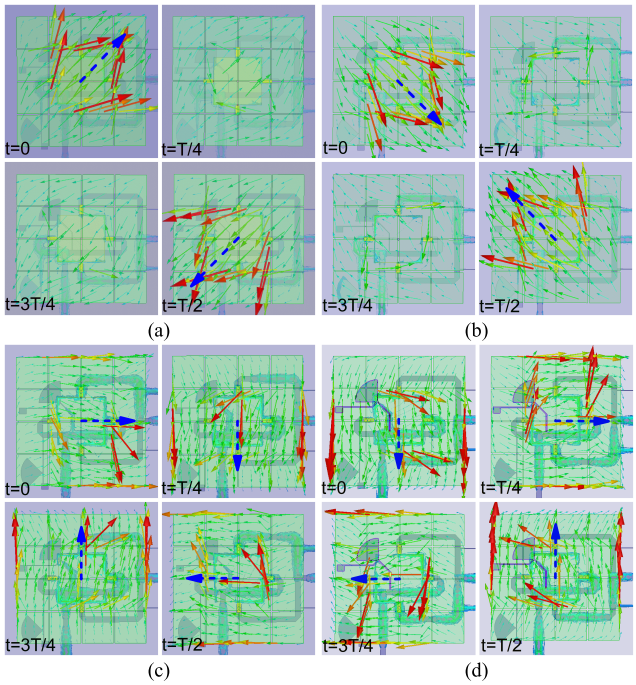

FIGURE 2. Simulated 5.6 GHz electric-field and surface current distributions of the designed metasurface antenna at four different time phases for the four polarization modes. (a) X-LP mode. (b) Y-LP mode. (c) LHCP mode. (d) RHCP mode.

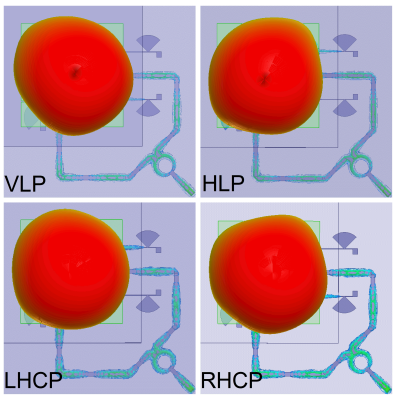

FIGURE 3. Simulated 5.6 GHz 3-D radiation patterns for the four polarization modes.

($\varphi = +45°$) for the X-LP mode are compared with the corresponding results in [24], as shown in Fig. 4. It can be easily demonstrated that the cross polarization level in the diagonal plane is significantly decreased. The other polarization states have similar results. The proposed metasurface antenna has a good polarization reconfigurable performance, and the full-wave simulated results for all polarization modes are presented and compared with the measured results in the following section.

III. SIMULATED AND MEASURED RESULTS

In order to validate the proposed concept, the designed prototype has been fabricated and measured. Fig. 5 shows the

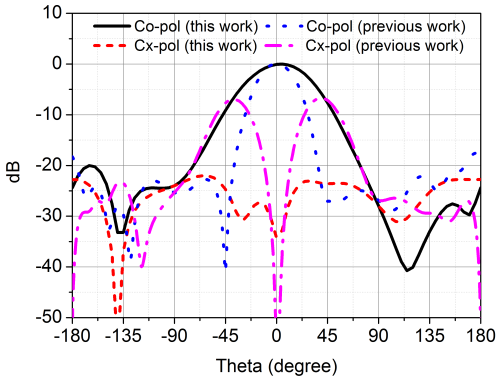

FIGURE 4. Simulated 5.6 GHz normalized radiation patterns in the diagonal plane for the X-LP mode.

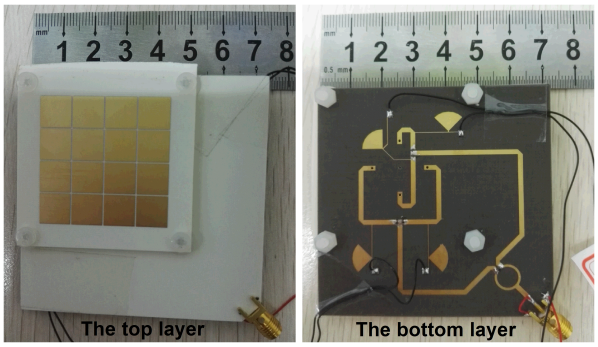

FIGURE 5. Photograph of the fabricated prototype.

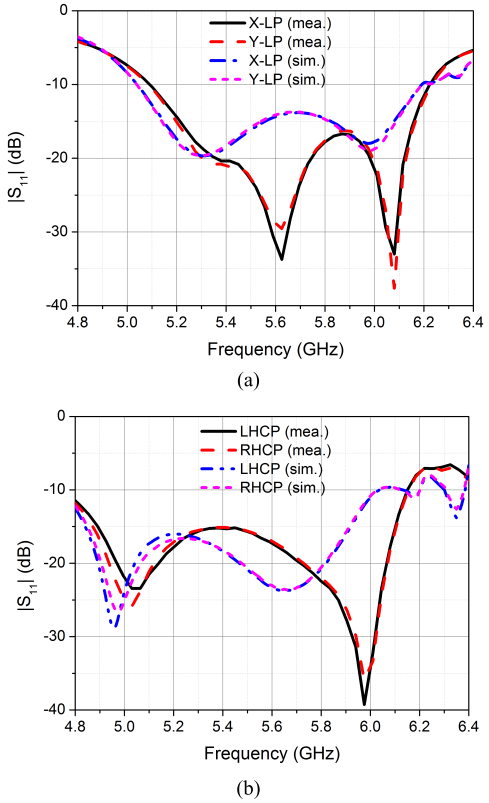

FIGURE 6. Measured and simulated reflection coefficients of the fabricated antenna. (a) X-LP and Y-LP modes. (b) LHCP and RHCP modes.

TABLE 3. Measured results of the polarization reconfigurable metasurface antenna.

Polarization state	X-LP	Y-LP	LHCP	RHCP
Impedance bandwidth (GHz)	5.1-6.22 (20%)	5.1-6.22 (20%)	4.75-6.15 (25%)	4.75-6.15 (25%)
Axial ratio bandwidth (GHz)	NON	NON	5.0-6.0 (17.8%)	5.0-6.06 (18.9%)
Maximum gain (dBi/dBic)	9.85	9.87	9.39	9.54
3 dB gain bandwidth (GHz)	5.05-6.35 (23.2%)	5.05-6.35 (23.2%)	5.05-6.15 (19.6%)	5.05-6.15 (19.6%)
Radiation efficiency at 5.6 GHz	76.2%	79.4%	68.4%	74.5%
Overlapped bandwidth (GHz)	5.1-6.22 (20%)	5.1-6.22 (20%)	5.05-6.0 (16.9%)	5.05-6.06 (18%)

prototype of the designed polarization reconfigurable metasurface antenna. Nylon bolts having 3mm diameter and plastic washers with thickness of 2 mm are used to support the metasurface layer. The reflection coefficients for all four polarization states are measured by the Agilent Vector Network Analyzer, and the measurements for far-field property are carried out in a microwave chamber. The fast rotating method [29], in which a fast rotating linearly polarized horn antenna is employed as a transmitting antenna, is adopted for the CP states.

The measured refection coefficients for the four states are compared with the corresponding simulated results in Fig. 6. It can be seen that the results for the two LP (CP) modes are almost the same due to the symmetry of antenna structure. The measured 10 dB return loss bandwidths are 5.1-6.22 GHz for the two LP modes and 4.75-6.16 GHz for the two CP modes.

The measured gains and AR properties for the four polarization states are presented in Fig. 7, where the corresponding simulated results are also included for comparison. The measured peak gains are 9.85 dBi, 9.87 dBi, 9.39 dBic and 9.54 dBic for X-LP, Y-LP, LHCP, RHCP modes, respectively, and the corresponding 3 dB gain bandwidths are 5.05-6.35 GHz (23.2%), 5.05-6.35 GHz (23.2%), 5.05-6.15 GHz (19.6%), and 5.05-6.15 GHz (19.6%). The measured gains are 0.8-1.5 dB smaller than that of the full wave simulated gains. This discrepancy is caused by the additional losses from the two SPDT switches, SMA connector and copper which are not taken into consideration in the full-wave simulation. The measured radiation efficiency, defined as the ratio of the measured gain to the simulated directivity, at 5.6 GHz for the four polarization modes are 76.2%, 79.4%, 68.4%, 74.5%, respectively. From Fig. 7(b) and (c), it can be seen that the measured 3 dB AR bandwidths are from 5.0 to 6.0 GHz (17.8%) for LHCP mode and from 5.0 to 6.06 GHz (18.9%) for RHCP mode, which has some differences with the full-wave simulated results. In the HFSS software, the PIN diodes are modeled as low-resistance (2-Ω) for ON state and open for OFF state. However, the accurate

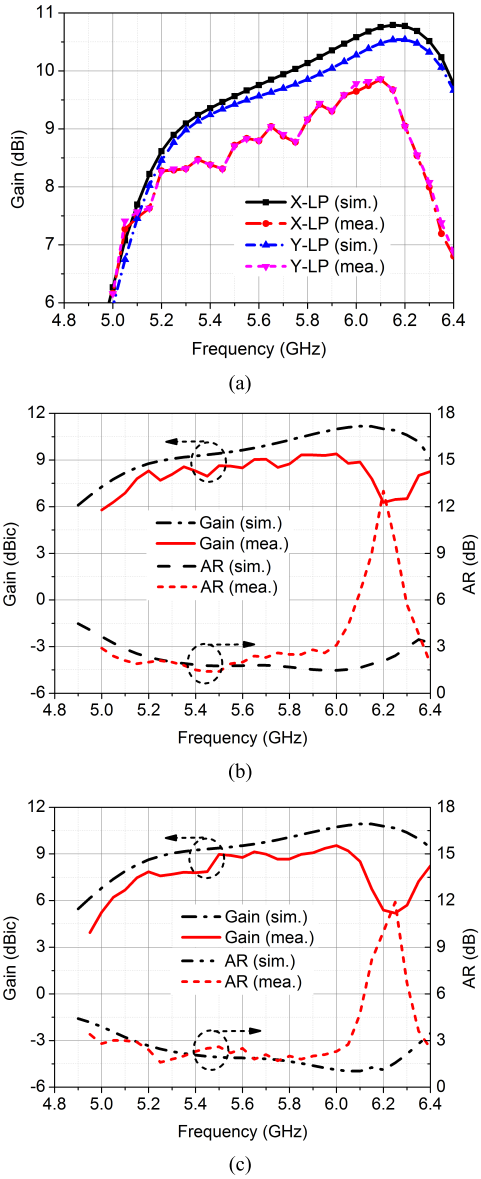

FIGURE 7. Measured and simulated gains and AR of the fabricated antenna. (a) X-LP and Y-LP modes. (b) LHCP mode. (c) RHCP mode.

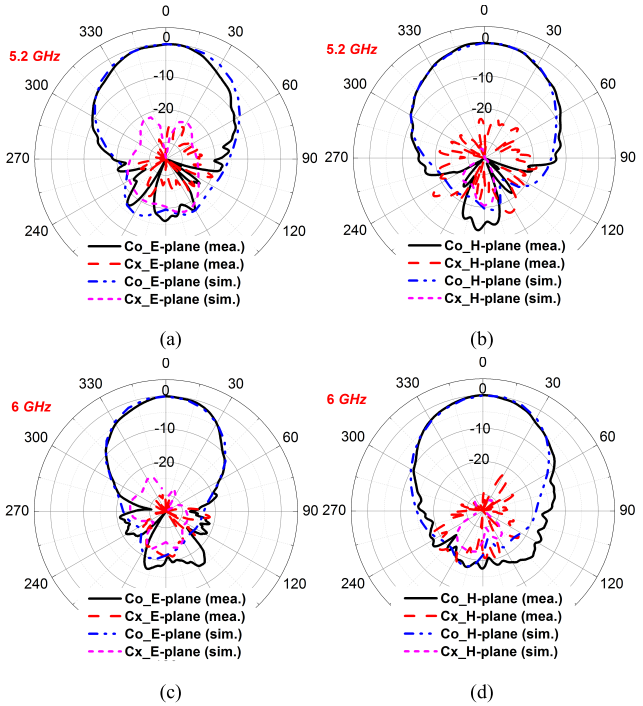

FIGURE 8. Measured and simulated normalized radiation patterns of the antenna array at X-LP mode. (a) E-plane at 5.2 GHz. (b) H-plane at 5.2 GHz. (c) E-plane at 6 GHz. (d) H-plane at 6 GHz.

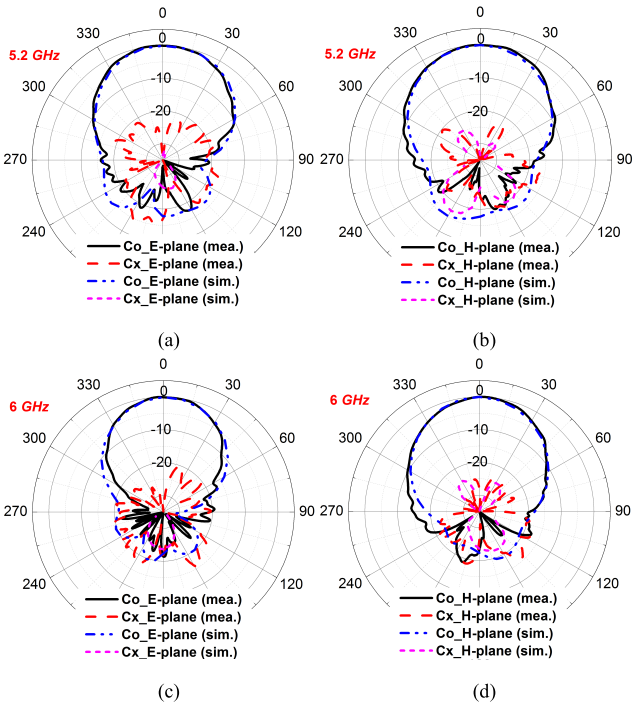

FIGURE 9. Measured and simulated normalized radiation patterns of the antenna array at Y-LP mode. (a) E-plane at 5.2 GHz. (b) H-plane at 5.2 GHz. (c) E-plane at 6 GHz. (d) H-plane at 6 GHz.

equivalent circuits for the PIN diodes are more complicated over the wide operating frequency band. At 6.2 GHz, the input impedances of the two paths have a big difference, which results in the imbalance of the power in the two paths. So the axial ratio is deteriorated. The measured results for the four polarization states, including operating bandwidths, peak gain, and radiation efficiency, are listed in Table III for more intuitive understanding.

The measured and simulated normalized radiation patterns at the two orthogonal cut-planes are compared at 5.2 and 6 GHz for the four polarizations modes, as shown in Figs. 8-11. Generally, the measured results are in good agreement with the simulated one for the all polarization states. For the two LP modes, the measured cross-polarization levels at both E- and H-plane are lower than −26 dB as shown in Figs. 8 and 9. From Figs. 10 and 11, it can be observed that the proposed antenna has good CP radiation properties at the two CP modes over a wide frequency band.

TABLE 4. Performance comparison with previously reported polarization reconfigurable antennas.

Reference	No. of Polarization States	Center Frequency (GHz)	Impedance Bandwidth (%)	3 dB AR Bandwidth (%)	Peak Gain (dBi/dBic)	Height (λ_0)	Total Size (λ_0^2)	No. of switches
[13]	V-LP, H-LP, LHCP, RHCP	2.44	18/30.7 (LP) 12.3/30.7 (CP)	4.5 (LHCP) 2.2 (RHCP)	6.2 (LP) 5.8 (CP)	0.042	n. a.	3 PIN diodes
[14]	LP, LHCP, RHCP	5	14.2 (LP) 26.4/26.4 (CP)	13.5 (LHCP) 13.5 (RHCP)	11.2	> 0.5	$1.83\lambda_0$*$1.83\lambda_0$	8 PIN diodes
[16]	LHCP, RHCP	1.85	80	37.8 (LHCP) 26.9 (RHCP)	4.8	Large	π*$(0.93\lambda_0)$ ^2	8 PIN diodes
[17]	LP, LHCP, RHCP	5.2	19.6	15.8	4.1 (LP) 4.25 (CP)	0.056	$0.9\lambda_0$*$0.9\lambda_0$	2 SPDTs, 1 SP3T
[19]	LP, LHCP, RHCP	3.5	22	11.4	7.5 (LP) 5 (CP)	0.018	π*$(0.9\lambda_0)$ ^2	mechanical
[22]	V-LP, H-LP, LHCP, RHCP	1.975	4.7/5.3 (LP) 3.5/3.5 (CP)	3.5 (LHCP) 3.8 (RHCP)	4 (LP) 4.5 (CP)	0.061	$0.5\lambda_0$*$0.5\lambda_0$	6 PIN diodes
[23]	V-LP, H-LP, LHCP, RHCP	0.93	6.1/7.5 (LP) 11/8.6 (CP)	1.7 (LHCP) 1.6 (RHCP)	7.98/7.82 (LP) 7.52/7.61 (CP)	0.034	$0.56\lambda_0$*$0.56\lambda_0$	8 PIN diodes
[24]	V-LP, H-LP, LHCP, RHCP	5.7	23.4/23.4 (LP) 27.2/27.2 (CP)	17.5 (LHCP) 19 (RHCP)	10.1/10.35 (LP) 9.9/9.85 (CP)	0.062	$2.64\lambda_0$*$2.83\lambda_0$	4 SPDTs
[30]	X-LP, Y-LP, LHCP, RHCP	2.3	less than 3.5	< 1	< 4.7 (LP) < 4.3 (CP)	0.01	$0.86\lambda_0$*$0.78\lambda_0$	48 PIN diodes
This work	X-LP, Y-LP, LHCP, RHCP	5.6	20/20 (LP) 25/25 (CP)	17.8 (LHCP) 18.9 (RHCP)	9.85/9.87 (LP) 9.39/9.54 (CP)	0.067	$1.3\lambda_0$*$1.3\lambda_0$	2 SPDTs

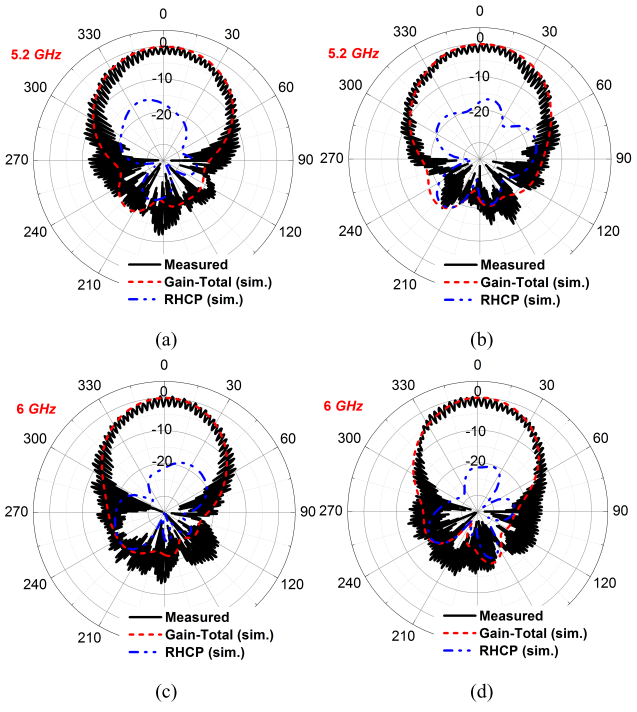

FIGURE 10. Measured and simulated normalized radiation patterns of the antenna array at LHCP mode. (a) horizontal plane at 5.2 GHz. (b) vertical plane at 5.2 GHz. (c) horizontal plane at 6 GHz. (d) vertical plane at 6 GHz.

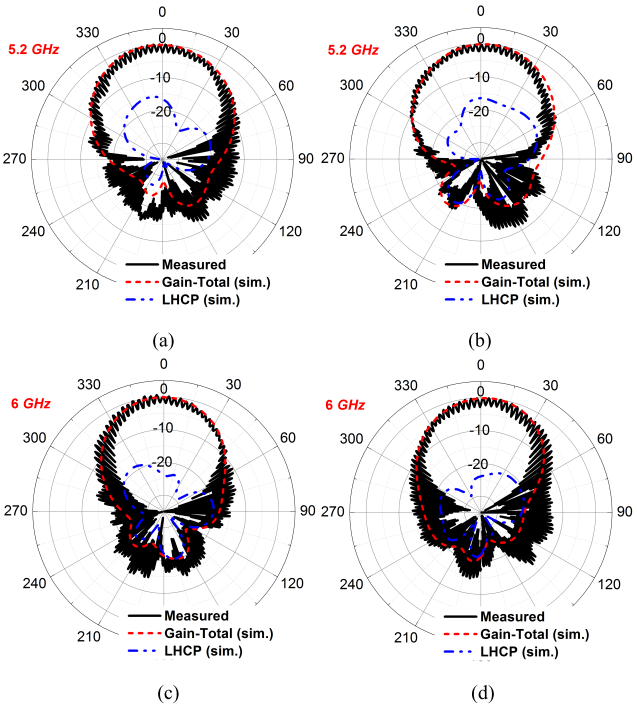

FIGURE 11. Measured and simulated normalized radiation patterns of the antenna array at RHCP mode. (a) horizontal plane at 5.2 GHz. (b) vertical plane at 5.2 GHz. (c) horizontal plane at 6 GHz. (d) vertical plane at 6 GHz.

Both the simulated and measured results show the good performance of the proposed polarization reconfigurable metasurface antenna, and the polarization of the antenna can be electrically switched among four polarization modes, including X-LP, Y-LP, LHCP, and RHCP, by controlling the states of the two SPDT switches. Moreover, the proposed antenna has a wide operating frequency band for all the polarization states. In addition, the feeding network and the dc bias circuit are designed on the bottom layer, which has little effect on the performance of the antenna.

Finally, the performance of some up-to-date polarization reconfigurable antennas and this work is summarized

in Table IV for comparison. Compared to our previous work [24], the antenna proposed in this paper has the same good performance using only two SPDT switches. In addition, the size of antenna is significantly reduced. From Table IV, it can be concluded that the proposed polarization reconfigurable metasurface antenna in this work has advantages of wide impedance bandwidth, wide AR bandwidth for CP modes, high enough gain and a low profile structure with four polarization states.

IV. CONCLUSION

To conclude, a low-profile wideband metasurface antenna with quad-polarization reconfiguration capability has been presented and designed in this paper. The four switchable feeding probes connected by two designed SPDT switches are introduced for achieving four polarization states. By controlling the states of the two SPDT switches, the operation of the proposed metasurface antenna can be switched among two orthogonal LP modes and two orthogonal CP modes. A prototype is fabricated and measured for the four polarization states, showing a reasonably agreement between the simulated and measured results. The proposed metasurface antenna has the advantages of low profile structure, quad-polarization reconfigurable ability, wide operating bandwidth, high enough gains as well as easiness of design and fabrication, and it can be potentially used for antenna polarization diversity application in the wireless systems.

ACKNOWLEDGMENT

The authors would like to thank T. Y. Huo and X. Q. Zhao with the State Key Laboratory of Millimeter Waves, Southeast University, Nanjing, China, for their kind help in prototype fabrication and measurement.

REFERENCES

[1] S. Xiao, C. Zheng, M. Li, J. Xiong, and B. Z. Wang, "Varactor-loaded pattern reconfigurable array for wide-angle scanning with low gain fluctuation," *IEEE Trans. Antennas Propag.*, vol. 63, no. 5, pp. 2364–2369, May 2015.

[2] Z.-C. Hao, H.-H. Wang, and W. Hong, "A novel planar reconfigurable monopulse antenna for indoor smart wireless access points' application," *IEEE Trans. Antenna Propag.*, vol. 64, no. 4, pp. 1250–1261, Apr. 2016.

[3] H. L. Zhu, X. H. Liu, S. W. Cheung, and T. I. Yuk, "Frequency-reconfigurable antenna using metasurface," *IEEE Trans. Antennas Propag.*, vol. 62, no. 1, pp. 80–85, Jan. 2014.

[4] X.-X. Yang, B.-C. Shao, F. Yang, A. Z. Elsherbeni, and B. Gong, "A polarization reconfigurable patch antenna with loop slots on the ground plane," *IEEE Antennas Wireless Propag. Lett.*, vol. 11, pp. 69–72, 2012.

[5] Y. Cao, S. W. Cheung, and T. I. Yuk, "A simple planar polarization reconfigurable monopole antenna for GNSS/PCS," *IEEE Trans. Antennas Propag.*, vol. 63, no. 2, pp. 500–507, Feb. 2015.

[6] J. F. Valenzuela-valdes, M. A. Garcia-fernandez, A. M. Martinez-Gonzalez, and D. Sanchez-Hernandez, "The role of polarization diversity for MIMO systems under Rayleigh-fading environments," *IEEE Antennas Wireless Propag. Lett.*, vol. 5, no. 1, pp. 534–536, Dec. 2006.

[7] S. Gao, A. Sambell, and S. S. Zhong, "Polarization-agile antennas," *IEEE Antennas Propag. Mag.*, vol. 48, no. 3, pp. 28–37, Jun. 2006.

[8] Y.-M. Cai, S. Gao, Y. Yin, W. Li, and Q. Luo, "Compact-size low-profile wideband circularly polarized omnidirectional patch antenna with reconfigurable polarizations," *IEEE Trans. Antennas Propag.*, vol. 64, no. 5, pp. 2016–2021, May 2016.

[9] J. M. Kovitz, H. Rajagopalan, and Y. Rahmat-Samii, "Design and implementation of broadband MEMS RHCP/LHCP reconfigurable arrays using rotated E-shaped patch elements," *IEEE Trans. Antennas Propag.*, vol. 63, no. 6, pp. 2497–2507, Jun. 2015.

[10] A. Khidre, K.-F. Lee, F. Yang, and A. Z. Elsherbeni, "Circular polarization reconfigurable wideband E-shaped patch antenna for wireless applications," *IEEE Trans. Antenna Propag.*, vol. 61, no. 2, pp. 960–964, Feb. 2013.

[11] M. S. Nishamol, V. P. Sarin, D. Tony, C. K. Aanandan, P. Mohanan, and K. Vasudevan, "An electronically reconfigurable microstrip antenna with switchable slots for polarization diversity," *IEEE Trans. Antenna Propag.*, vol. 59, no. 9, pp. 3424–3427, Sep. 2011.

[12] Z.-X. Yang, H.-C. Yang, J.-S. Hong, and Y. Li, "Bandwidth enhancement of a polarization-reconfigurable patch antenna with stair-slots on the ground," *IEEE Antennas Wireless Propag. Lett.*, vol. 13, pp. 579–582, 2014.

[13] R.-H. Chen and J.-S. Row, "Single-fed microstrip patch antenna with switchable polarization," *IEEE Trans. Antenna Propag.*, vol. 56, no. 4, pp. 922–926, Apr. 2008.

[14] L.-Y. Ji, P.-Y. Qin, Y. J. Guo, C. Ding, G. Fu, and S.-X. Gong, "A wideband polarization reconfigurable antenna with partially reflective surface," *IEEE Trans. Antenna Propag.*, vol. 64, no. 10, pp. 4534–4538, Oct. 2016.

[15] S. W. Lee and Y. J. Sung, "Simple polarization-reconfigurable antenna with T-shaped feed," *IEEE Antennas Wireless Propag. Lett.*, vol. 15, pp. 114–117, 2016.

[16] W. Lin and H. Wong, "Wideband circular polarization reconfigurable antenna," *IEEE Trans. Antenna Propag.*, vol. 63, no. 12, pp. 5938–5944, Dec. 2015.

[17] W. Yang, W. Che, H. Jin, W. Feng, and Q. Xue, "A polarization-reconfigurable dipole antenna using polarization rotation AMC structure," *IEEE Trans. Antenna Propag.*, vol. 63, no. 12, pp. 5305–5315, Dec. 2015.

[18] J. Hu, Z. C. Hao, and Z. W. Miao, "Design and implementation of a planar polarization-reconfigurable antenna," *IEEE Antennas Wireless Propag. Lett.*, vol. 16, pp. 1557–1560, 2017.

[19] H. L. Zhu, S. W. Cheung, X. H. Liu, and T. I. Yuk, "Design of polarization reconfigurable antenna using metasurface," *IEEE Trans. Antennas Propag.*, vol. 62, no. 6, pp. 2891–2898, Jun. 2014.

[20] Y. F. Wu, C. H. Wu, D. Y. Lai, and F. C. Chen, "A reconfigurable quadri-polarization diversity aperture-coupled patch antenna," *IEEE Trans. Antennas Propag.*, vol. 55, no. 3, pp. 1009–1012, Mar. 2007.

[21] F. Ferrero, C. Luxey, R. Staraj, G. Jacquemod, M. Yedlin, and V. Fusco, "A novel quad-polarization agile patch antenna," *IEEE Trans. Antennas Propag.*, vol. 57, no. 5, pp. 1563–1567, May 2009.

[22] J.-S. Row and M.-J. Hou, "Design of polarization diversity patch antenna based on a compact reconfigurable feeding network," *IEEE Trans. Antenna Propag.*, vol. 62, no. 10, pp. 5349–5352, Oct. 2014.

[23] H. Sun and S. Sun, "A novel reconfigurable feeding network for quad-polarization agile antenna design," *IEEE Trans. Antenna Propag.*, vol. 64, no. 1, pp. 311–316, Jan. 2016.

[24] J. Hu, Z.-C. Hao, and W. Hong, "Design of a wideband quad-polarization reconfigurable patch antenna array using a stacked structure," *IEEE Trans. Antenna Propag.*, vol. 65, no. 6, pp. 3014–3023, Jun. 2017.

[25] W. Yang, J. Zhou, Z. Yu, and L. Li, "Single-fed low profile broadband circularly polarized stacked patch antenna," *IEEE Trans. Antenna Propag.*, vol. 62, no. 10, pp. 5406–5410, Oct. 2014.

[26] MACOM Company. *MADP-000907-14020P PIN Diode*. Accessed: Jan. 5, 2017. [Online]. Available: http://www.macom.com/products/product-detail/MADP-000907-14020P

[27] S. X. Ta and I. Park, "Low-profile broadband circularly polarized patch antenna using metasurface," *IEEE Trans. Antennas Propag.*, vol. 63, no. 12, pp. 5929–5934, Dec. 2015.

[28] F. Costa, O. Luukkonen, C. R. Simovski, A. Monorchio, S. A. Tretyakov, and P. M. de Maagt, "TE surface wave resonances on high-impedance surface based antennas: Analysis and modeling," *IEEE Trans. Antennas Propag.*, vol. 59, no. 10, pp. 3588–3596, Oct. 2011.

[29] B. Y. Toh, R. Cahill, and V. F. Fusco, "Understanding and measuring circular polarization," *IEEE Trans. Educ.*, vol. 46, no. 3, pp. 313–318, Aug. 2003.

[30] L. Ge, Y. Li, J. Wang, and C.-Y.-D. Sim, "A low-profile reconfigurable cavity-backed slot antenna with frequency, polarization, and radiation pattern agility," *IEEE Trans. Antenna Propag.*, vol. 65, no. 5, pp. 2182–2189, May 2017.

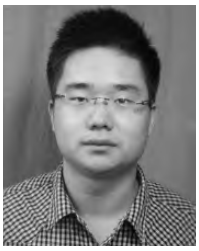

JUN HU (S'17) received the B.S. degree in electronics and information engineering from Anhui Agricultural University, Hefei, China, in 2012, and the M.S. degree in electromagnetic field and microwave technology from Southeast University, Nanjing, China, in 2014, where he is currently pursuing the Ph.D. degree in electronic science and technology.

His recent research interests include the design of tunable devices, passive components, reconfigurable antennas, and antenna array.

GUO QING LUO (M'08) received the B.S. degree from the China University of Geosciences, Wuhan, in 2000, the M.S. degree from Northwest Polytechnical University, Xi'an, China, in 2003, and the Ph.D. degree from Southeast University, Nanjing, China, in 2007.

Since 2007, he has been with the faculty of the School of Electronics and Information, Hangzhou Dianzi University, as a Lecturer, and was promoted to Professor in 2011. He holds 16 Chinese patents and has authored or co-authored 65 technical papers in referred journals and conferences. His current research interests include RF, microwave and millimeter-wave passive devices, antennas, and frequency selective surfaces.

Dr. Luo is a member of the IEEE Antennas and Propagation Society and Microwave Theory and Techniques Society. He was a recipient of the CST University Publication Award in 2007, the National Excellent Doctoral Dissertation of China in 2009, and the National Natural Science Award (the second class) of China in 2016.

ZHANG-CHENG HAO (M'08–SM'15) received the B.S. degree in microwave engineering from Xidian University, Xi'an, China, in 1997, and the M.S. and Ph.D. degrees in radio engineering from Southeast University, Nanjing, China, in 2002 and 2006, respectively.

In 2006, he was a Post-Doctoral Researcher with the Laboratory of Electronics and Systems for Telecommunications, École Nationale Supérieure des Télécommunications de Bretagne, Bretagne, France, where he was involved with developing millimeter-wave antennas. In 2007, he joined the Department of Electrical, Electronic and Computer Engineering, Heriot-Watt University, Edinburgh, U.K., as a Research Associate, where he was involved with developing multilayer integrated circuits and ultra-wide-band components. In 2011, he joined the School of Information Science and Engineering, Southeast University, Nanjing, as a Professor. He holds 20 granted patents and has authored and co-authored over 150 referred journal and conference papers. His current research interests involve microwave and millimeter-wave systems, submillimeter-wave and terahertz components and passive circuits, including filters, antenna arrays, couplers, and multiplexers.

Dr. Hao has served as the reviewer for many technique journals, including the IEEE TRANSACTIONS ON MICROWAVE THEORY AND TECHNIQUES, the IEEE TRANSACTIONS ON ANTENNAS AND PROPAGATION, the IEEE ANTENNAS AND WIRELESS PROPAGATION LETTERS, and the IEEE MICROWAVE AND WIRELESS COMPONENTS LETTERS. He was a recipient of the Thousands of Young Talents presented by China government in 2011 and the High Level Innovative and Entrepreneurial Talent presented by Jiangsu, China, in 2012.